

1 **Real-time measurement of pelvis and trunk kinematics during treadmill locomotion**
2 **using a low-cost depth-sensing camera: A concurrent validity study**
3

4 Short Communication

5

6 Tom W. Macpherson¹, Jonathan Taylor¹, Thomas McBain¹, Matthew Weston¹ and Iain R. Spears¹

7

8 ¹School of Social Sciences Business and Law, Teesside University, Middlesbrough, UK.

9

10 **Corresponding Author:** Tom W. Macpherson

11 Sport and Exercise Subject Group, School of Social Sciences,
12 Business and Law, Teesside University, Middlesbrough, UK.

13 E-mail: t.macpherson@tees.ac.uk

14 **Abstract Word Count:** 249

15 **Text Word Count:** 2034

16 **Number of Figures:** 2

17 **Number of Tables:** 3

18 **Abstract**

19 There is currently no suitable kinematic system for a large-scale prospective trial assessing
20 risk factors of musculoskeletal disorders. A practical kinematic system is described which
21 involves the use of a single low-cost depth-sensing camera for the real-time measurement of
22 3-dimensional linear and angular pelvic and trunk range-of-movement (ROM). The method is
23 based on the creation and processing of dynamic point clouds taken from the posterior
24 surface of the pelvis and trunk. Nine healthy participants performed 3 trials of treadmill
25 locomotion when walking at self-selected speed (3.6-5.6 km/h), running at 70% (10.9-14.0
26 km/h) and 90% of maximal speed (14.0-18.0 km/h). Stride-by-stride linear and angular ROM
27 data were captured concurrently using the single depth-sensing camera running at 30Hz
28 (Kinect™ for Windows, Microsoft, USA) and a six-camera motion capture system at 100Hz
29 (Vicon MX13, Vicon Motion Systems, United Kingdom). Within subject correlation
30 coefficients between the practical and criterion method ranged from very large to nearly
31 perfect ($r = 0.87-1.00$) for the linear ROM. Correlation coefficients for the angular ROM
32 ranged from moderate to very large ($r = 0.41-0.80$). The limits of agreement between the two
33 systems for linear movements was ≤ 9.9 mm at all velocities of gait and ≤ 4.6 degrees at all
34 velocities of gait. The single camera system using depth-sensing technology is capable of
35 capturing linear pelvic and trunk ROM during treadmill locomotion with reasonable precision
36 when compared to the criterion method. Further improvements to the measurement of angles
37 and validation across a wider population are recommended.

1. Introduction

39 Biofeedback is an emerging tool in the management of injuries in at-risk groups. When a
40 biomechanical risk factor can be quantified and displayed to the participant it is possible to
41 address the underlying biomechanical problem (Crowell and Davis, 2011). The quantification
42 of risk factor variables requires a prospective study in which measurements are made in
43 injury-free participants at baseline, thus allowing modelling to take place in the follow-up
44 period. The strength of such statistical models depends on the number of injury events
45 occurring in the follow-up period. Hence, large-scale baseline trials are a prerequisite even
46 when considering the more common musculoskeletal injuries (e.g. iliotibial band syndrome).

47 The pelvic and trunk regions form the proximal end of the lower kinetic chain and are
48 routinely assessed due to their reputed relationship with pelvic, spinal and lower limb
49 pathologies (Liebenson, 2004; Sahrman, 2002; Herrington, 2011). The surrounding core
50 musculature provides the control and stabilization necessary for efficient gait with abnormal
51 linear and/or angular oscillations of the pelvic and trunk regions during gait being implicated
52 in, or symptomatic of, many musculoskeletal conditions (Saunders et al., 2005). An
53 accessible, valid and real-time method of kinematic analysis for quantifying pelvic and trunk
54 movements may therefore be a useful tool in injury research (Vieira and Kumar, 2004; Dutta,
55 2012). To date several studies have presented protocols to quantify pelvic movements during
56 gait (Schache et al., 2002a; Schache et al., 2000). However, these are lab-based and time-
57 consuming in terms of preparation, collection and analysis and restricted to relatively small-
58 scale trials.

59 Depth-sensing cameras, such as the Kinect sensor (Microsoft™, USA), may offer an
60 affordable and pragmatic alternative (Dutta, 2012). The Kinect sensor allows depth and
61 infrared images (640 by 480 pixels) to be collected simultaneously at 30 Hz with each pixel
62 representing about 0.09 degrees in the image plane. The depth data, with an error ranging
63 from less than 0.2 mm at small (0.4 m) distances to 4 cm at large distances (5 m)
64 (Khoshelham & Elberink, 2012), are more precise than the better known skeletal tracking
65 data (Dutta, 2012). These depth arrays are currently being used in a range of disciplines and
66 recently in biomechanics research to measure foot kinematics (van den Herrewegen et al.,
67 2014).

68 The aim of this study is to develop and evaluate the use of a single-camera system, based on
69 this technology, to quantify the 3-dimensional kinematics of the pelvic and trunk regions
70 during treadmill locomotion.

71 2. Methods

72 Nine male participants volunteered for the study (age 29.2 ± 4.2 y, height 182.9 ± 7.3 cm,
73 mass 84.5 ± 10.4 kg and body mass index 25.3 ± 3.1 kg/m²). The participants had no prior or
74 existing lower limb injury or neurological disorder affecting gait. Ethical approval was
75 obtained from Teesside University and written informed consent was obtained from all
76 participants. Participants attended the laboratory on two occasions. First, they undertook the
77 30-15 Intermittent Fitness Test (30-15 IFT) (Buchheit, 2005) which allowed the
78 determination of appropriate running speeds for the experimental trial by recording the
79 maximum running velocity reached at the end of the test (VIFT). On the second visit,
80 participants completed trials (180s each) at 3 different speeds of locomotion which were:
81 walking at self-selected speed (3.6-5.6 km/h), running at 70% of VIFT (10.9-14.0 km/h) and
82 running at 90% of VIFT (14.0-18.0 km/h).

83 The depth-sensing camera (Kinect™ for Windows, Version 1, Microsoft, USA) projects a
84 structured grid of infrared light into the field of view. The system is pre-programmed to
85 triangulate the reflections of this grid in order to determine camera-object distances on a
86 pixel-by-pixel basis. Our algorithm for 3-dimensional measurement involved the creation of a
87 point cloud around the region of interest. In this example, retro-reflective markers (Figure 1a)
88 were used to create overexposed effects on the infrared image (Figure 1bi), thus allowing
89 marker centroids to be determined on a frame-by-frame basis using standard threshold
90 procedures. Starting five pixels above the centroid, four scanlines (two vertical and two
91 horizontal) were superimposed on the depth image (Figure 1bi). The depth data along these
92 scanlines were then used to create a 42 point cloud around each marker (Figure 1bii, iii and
93 iv) with the mean depth being used as the camera-marker distance (Z_L [Figure 1a]). Using
94 trigonometry and field of view information supplied by the manufacturer (43 degrees vertical
95 and 57 degrees horizontal), the medial-lateral (X_L) and superior-inferior (Z_L) positions of the
96 marker were calculated for all markers. The tracked data from the single-camera system was
97 to be compared with concurrently collected data from a commercially available six-camera
98 motion capture solution (Vicon MX13 and Vicon Nexus 1.7, Vicon Motion Systems, UK).
99 The six-camera system is a passive video based 3D motion capture system which was
100 calibrated prior to every session, following manufacturers' guidelines, to ensure image error
101 was below 0.18 mm.

102 In order to run both systems concurrently for the treadmill trials some compromises on the
103 quality of the angular data had to be made. Notably, a commonly accepted model for the 3-
104 dimensional kinematics of the pelvis (e.g. Kadaba et al. 1990) was not feasible due to
105 occlusion of the anterior markers by the arms, adipose tissue and the treadmill safety guard.
106 An alternative approach using a posteriorly positioned cluster of orthogonally positioned
107 markers (Borhani et al., 2013) was tested but our tracking algorithm lacked the elegance to
108 separate very closely-positioned markers. Subsequently, we therefore had to compromise on
109 quality of the data by using just two markers (30 mm in diameter) on each of the posterior
110 iliac spines and on each of the tenth ribs (Figure 1a). For both systems, the linear positions of
111 the pelvis and trunk were defined as the mid-points of the vectors joining left- and right-sided
112 markers. Angular positions were recorded as the angles these vectors made relative to the X-
113 axis when projected onto the global XY and XZ planes (Figure 1a). These measures are
114 proxy measures of rotation and obliquity, respectively. Unfortunately, it was not possible to
115 derive measures of pelvic tilt (i.e. sagittal plane movements) or Euler angles as suggested by
116 Wu et al. (2002). This approach did, however, allow us to assess the potential of this simple
117 device for deriving angular data in addition to linear data.

118 Sampling frequency for the six-camera system was 100Hz and data from the single-camera
119 (approximately 30Hz) were upsampled to 100Hz using linear interpolation. Cameras for the
120 six-camera system were set at a height of 1.9 m. The height of the single-camera was 1.6 m
121 (i.e. approximately the same level of the participants' posterior-superior iliac spines when
122 standing on the treadmill). The distance between the single-camera system and the participant
123 was between 1.0-3.6 m to ensure the highest quality field of view while maintaining accuracy
124 (Dutta, 2012). For comparison purposes, an angular ($+90^\circ$, $+180^\circ$, 0°) and linear
125 transformation using the position of the single-camera in the global frame were applied to the
126 data from the single camera system. The time-series over a 10 second period for the triaxial
127 linear (Figure 2a, b and c) and biplanar angular (Figure 2d and e) data were used to determine
128 the range-of-movements (ROM) on a stride-by-stride basis. Specifically, the beginning of a
129 gait cycle was identified at every 2nd point of inflexion on the superior-inferior time-series
130 for the pelvis (Figure 2b).

131 A within-subject design (Weston et al., 2014) was used to determine the association between
132 the ROM data for the single- and six-camera systems. This design permits the analysis of
133 within-subject changes by removing between-subject differences (Bland and Altman, 1995).
134 Confidence limits (90%) for the within-subject correlations were calculated as per Altman
135 and Bland (2011). The following scale of magnitudes was used to interpret the magnitude of
136 the correlation coefficients: <0.1, trivial; 0.1–0.3, small; 0.3–0.5, moderate; 0.5–0.7, large;
137 0.7–0.9, very large; >0.9, nearly perfect (Hopkins et al., 2009). Limits of Agreement (LoA)
138 (Bland and Altman, 1986) were also used to assess the agreement between the single- and
139 six-camera systems. This method allows for the systematic and random error to be analysed
140 between the two systems (Giavarina, 2015).

141 **3. Results**

142 All within subject correlations for the single- and six-camera systems are displayed in Table
143 1. Within subject correlations for the association between the single- and six-camera systems
144 when examining the linear ROM of the pelvis were nearly perfect for all directions and
145 speeds with the exception of the ROMs recorded in the anterior-posterior direction at the
146 fastest speed, which was very large ($r = 0.89$, 90% Confidence Limit: 0.76-0.96). Similarly,
147 nearly perfect correlations were found for the trunk with the exceptions of anterior-posterior
148 movements when running at 70% of VIFT ($r=0.90$, CL: 0.76-0.96) and 90% of VIFT ($r =$
149 0.87 , CL: 0.71-0.95). The correlations between the two systems in terms of angular ROMs
150 were less consistent ranging from moderate to large at self-selected walking and large to very
151 large when running. The agreement between the two systems (Table 2) for linear movements
152 is ≤ 9.9 mm at all velocities of gait and ≤ 4.6 degrees at all velocities of gait. Descriptive data
153 for the absolute linear and angular ROM for both systems are presented in Table 3.

154 **4. Discussion**

155 This study is based on the premise that kinematic data of the pelvis and trunk could
156 contribute to injury management and may facilitate gait retraining (e.g. Sharma et al., 2014;
157 Crowell and Davis, 2011). To do so, requires a prospective study which in turn requires a
158 system which is safe, rapid, easy-to-use and portable. The single-camera system described in
159 this study meets these requirements and the data it produces compares reasonably well with
160 the six-camera system for the degrees of freedoms tested. In addition, the absolute values
161 reported are comparable with previous literature. Superior-inferior and medial-lateral
162 movements of the pelvis (mean ROM 4.7 cm and 5.0 cm, respectively) during walking were
163 within the ranges (2.5–9.5 cm and 2.0–6.0 cm) reported by Thorstensson et al. (1982),
164 although the anterior-posterior movements (3.9 cm) were slightly higher. Transversal pelvic
165 rotations during walking (6.3 ± 1.8 degrees) match those reported by Staszkiwicz et al.
166 (2012) (6.3 ± 2.5 degrees) for treadmill walking at 5 km/h. Similarly transversal pelvic
167 rotations during running (9.3 ± 2.1 degrees) were within the range reported in previous
168 studies (Kadaba et al., 1990; Saunders et al., 2005). Consistent with previous studies
169 (Saunders et al., 2005 and Crosbie et al., 1997), the data from the two systems showed
170 increases in ROM of the pelvic and trunk motion in all planes with an increase in walking
171 and running speed. Taken together this practical system may provide a useful tool for the
172 objective assessment of the pelvis and trunk during treadmill locomotion.

173 There are important limitations with the current system and also with the research design.
174 Despite reasonable agreement between the two systems in terms of angular ROM, it should
175 be reiterated that the variables being reported here are necessarily simplified and do not meet
176 the accepted standards (Wu et al., 2002). To address this shortfall in future will require

177 additional markers, which in turn will necessitate improved tracking algorithms and/or
178 additional sensors (e.g. Buganè et al., 2014). In order to ensure that intra-marker distances
179 remain sufficient to avoid accentuating angular error it may be necessary to find new marker
180 locations or improved versions of the camera (i.e. with a higher resolution). Secondly, it
181 should also be noted that the single-camera system described in this study has been created
182 specifically for the analysis of upright treadmill locomotion and thus could not be used for
183 more complex movements. Thirdly, our sample was fairly homogeneous in terms of
184 anthropometric variables and the system would need to be tested in a wider population which
185 may include clinical or obese populations, for whom small abnormal movements and skin
186 movements may be much more problematic (Schache et al., 2002b). Nonetheless, the
187 posterior approach to measurement, as used in this system, appears to be more reliable than
188 traditional kinematic models for these populations (Borhani et al., 2013).

189 In conclusion, this study has shown that the single depth-sensing camera system offers a
190 pragmatic method for kinematic capture of the pelvic and trunk regions for most of the
191 degrees of freedom tested. However, further research to address the highlighted limitations is
192 recommended before being used for large-scale data collection and biofeedback applications.

193 **Conflict of interest statement**

194 None of the authors have a conflict of interest related to this work.

195 **Acknowledgements**

196 This work is based on algorithms developed for a Research Councils UK Research in the
197 Wild.

198
199
200
201
202
203
204
205
206
207
208
209
210
211
212
213
214
215
216
217
218
219
220
221
222
223
224
225
226

227 **References**

- 228 • Altman, D.G. & Bland, J.M. (2011). How to obtain the P value from a confidence
229 interval. *British Medical Journal*, 343.
- 230 • Bland, J. M., & Altman, D. (1986). Statistical methods for assessing agreement
231 between two methods of clinical measurement. *The Lancet*, 327(8476), 307-310.
- 232 • Bland, J.M. & Altman, D.G. (1995) Calculating correlation coefficients with
233 repeated observations: Part 2—Correlation between subjects. *British Medical*
234 *Journal*, 310(6980), 633.
- 235 • Borhani, M., McGregor, A. H. & Bull, A. M. (2013) An alternative technical
236 marker set for the pelvis is more repeatable than the standard pelvic marker set.
237 *Gait & posture*, 38(4), 1032-1037.
- 238 • Buchheit, M. (2005) The 30-15 Intermittent Fitness Test: a new intermittent
239 running field test for intermittent sport players-Part 1. *Approches du Handball*, 87,
240 27-34.
- 241 • Buganè, F., Benedetti, M. G., D'Angeli, V. & Leardini, A. (2014) Estimation of
242 pelvis kinematics in level walking based on a single inertial sensor positioned
243 close to the sacrum: validation on healthy subjects with stereo photogrammetric
244 system. *Biomedical engineering online*, 13(1), 146.
- 245 • Crosbie, J., Vachalathiti, R. & Smith, R. (1997) Age, gender and speed effects on
246 spinal kinematics during walking. *Gait & Posture*, 5(1), 13-20.
- 247 • Crowell, H.P. & Davis I.S. (2011) Gait retraining to reduce lower extremity
248 loading in runners. *Clinical Biomechanics*, 26(1), 78-83.
- 249 • Dutta, T. (2012) Evaluation of the Kinect™ sensor for 3-D kinematic
250 measurement in the workplace. *Applied ergonomics*, 43(4), 645-649.
- 251 • Giavarina, D. (2015). Understanding Bland Altman analysis. *Biochemia medica*,
252 25(2), 141-151.
- 253 • Herrington, L. (2011) Assessment of the degree of pelvic tilt within a normal
254 asymptomatic population. *Manual therapy*, 16(6), 646-648.
- 255 • Hopkins, W., Marshall, S., Batterham, A. & Hanin, J. (2009) Progressive statistics
256 for studies in sports medicine and exercise science. *Medicine+ Science in Sports+*
257 *Exercise*, 41(1), 3.
- 258 • Kadaba, M. P., Ramakrishnan, H. K. & Wootten, M. E. (1990) Measurement of
259 lower extremity kinematics during level walking. *Journal of orthopaedic research*,
260 8(3), 383-392.
- 261 • Khoshelham, K., & Elberink, S.O. (2012) Accuracy and resolution of kinect depth
262 data for indoor mapping applications. *Sensors*, 12(2), 1437-1454.
- 263 • Liebenson, C. (2004) The relationship of the sacroiliac joint, stabilization
264 musculature, and lumbo-pelvic instability. *Journal of bodywork and movement*
265 *therapies*, 8(1), 43-45.
- 266 • Sahrman, S. (2002) Diagnosis and treatment of movement impairment
267 syndromes. Elsevier Health Sciences.
- 268 • Saunders, S.W., Schache, A., Rath, D. & Hodges, P.W. (2005) Changes in three
269 dimensional lumbo-pelvic kinematics and trunk muscle activity with speed and
270 mode of locomotion. *Clinical Biomechanics*, 20(8), 784-793.
- 271 • Schache, A.G., Blanch, P.D. & Murphy, A.T. (2000) Relation of anterior pelvic
272 tilt during running to clinical and kinematic measures of hip extension. *British*
273 *journal of sports medicine*, 34(4), 279-283.

- 274
- 275
- 276
- 277
- 278
- 279
- 280
- 281
- 282
- 283
- 284
- 285
- 286
- 287
- 288
- 289
- 290
- 291
- 292
- 293
- 294
- 295
- 296
- 297
- 298
- 299
- 300
- 301
- 302
- 303
- 304
- 305
- 306
- Schache, A.G., Blanch, P.D., Rath, D., Wrigley, T. & Bennell, K. (2002a). Three-dimensional angular kinematics of the lumbar spine and pelvis during running. *Human Movement Science*, 21(2), 273-293.
 - Schache, A.G., Blanch, P.D., Rath, D.A., Wrigley, T.V., Starr, R. & Bennell, K.L. (2002b) Intra-subject repeatability of the three dimensional angular kinematics within the lumbo–pelvic–hip complex during running. *Gait & posture*, 15(2), 136-145.
 - Sharma, J., Weston, M., Batterham, A.M. & Spears, I.R. (2014) Gait Retraining and Incidence of Medial Tibial Stress Syndrome in Army Recruits. *Medicine and Science in Sports and Exercise*, 46 (9), pp. 1684-1692.
 - Staszkiwicz, R., CHWAŁA, W., Forczek, W. & Laska, J. (2012) Three-dimensional analysis of the pelvic and hip mobility during gait on a treadmill and on the ground. *Mechanics*, 1, 12.
 - Thorstensson, A., Carlson, H., Zomlefer, M. R. & Nilsson, J. (1982) Lumbar back muscle activity in relation to trunk movements during locomotion in man. *Acta Physiologica Scandinavica*, 116(1), 13-20.
 - Van den Herrewegen, I., Cuppens, K., Broeckx, M., Barisch-Fritz, B., Vander Sloten, J., Leardini, A. & Peeraer, L. (2014) Dynamic 3D scanning as a markerless method to calculate multi-segment foot kinematics during stance phase: Methodology and first application. *Journal of biomechanics*, 47(11), 2531-2539.
 - Vieira, E.R. & Kumar, S. (2004) Working postures: a literature review. *Journal of Occupational Rehabilitation*, 14(2), 143-159.
 - Weston, M., Siegler, J., Bahnert, A., McBrien, J. & Lovell, R. (2014) The application of differential ratings of perceived exertion to Australian Football League matches. *Journal of Science and Medicine in Sport*. [doi:10.1016/j.jsams.2014.09.001](https://doi.org/10.1016/j.jsams.2014.09.001)
 - Wu, G., Siegler, S., Allard, P., Kirtley, C., Leardini, A., Rosenbaum, D., Whittle, M., D’Lima, D.D., Cristofolini, L., Witte, H., Schmid, O. & Stokes, I. (2002) ISB recommendation on definitions of joint coordinate system of various joints for the reporting of human joint motion—part I: ankle, hip, and spine. *Journal of biomechanics*, 35(4), 543-548.

307

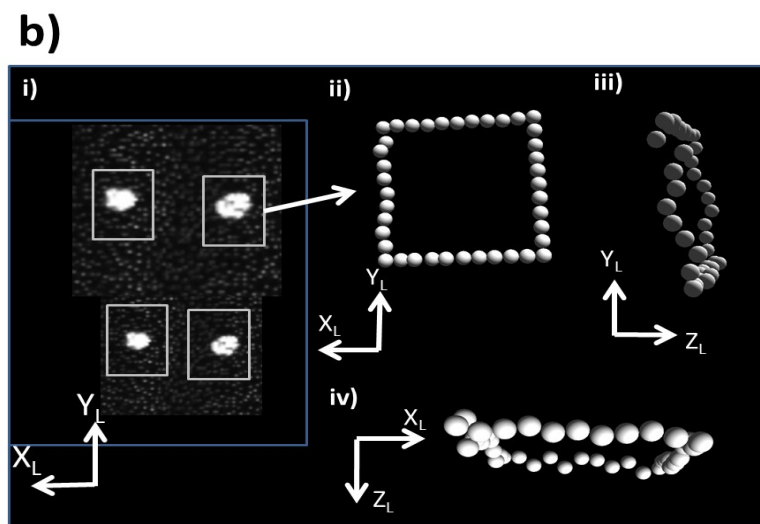
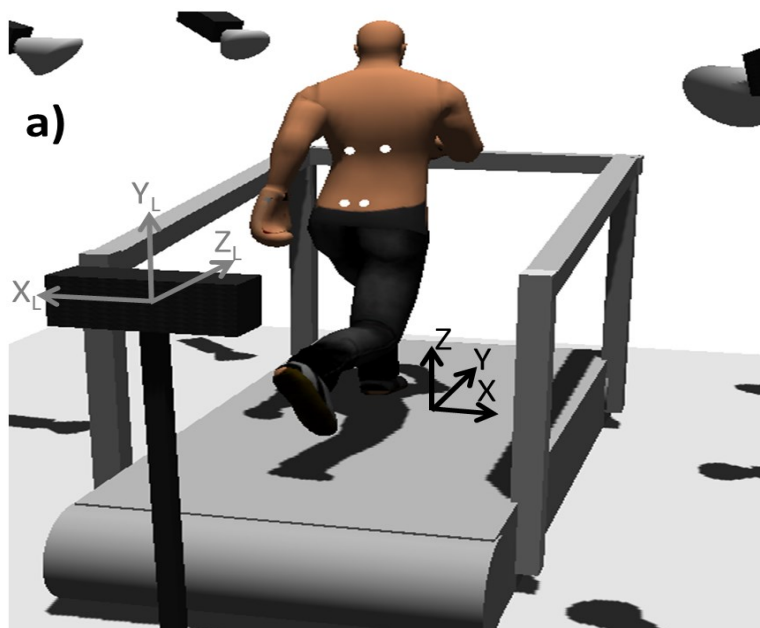
308

309

310

311

312



313
314

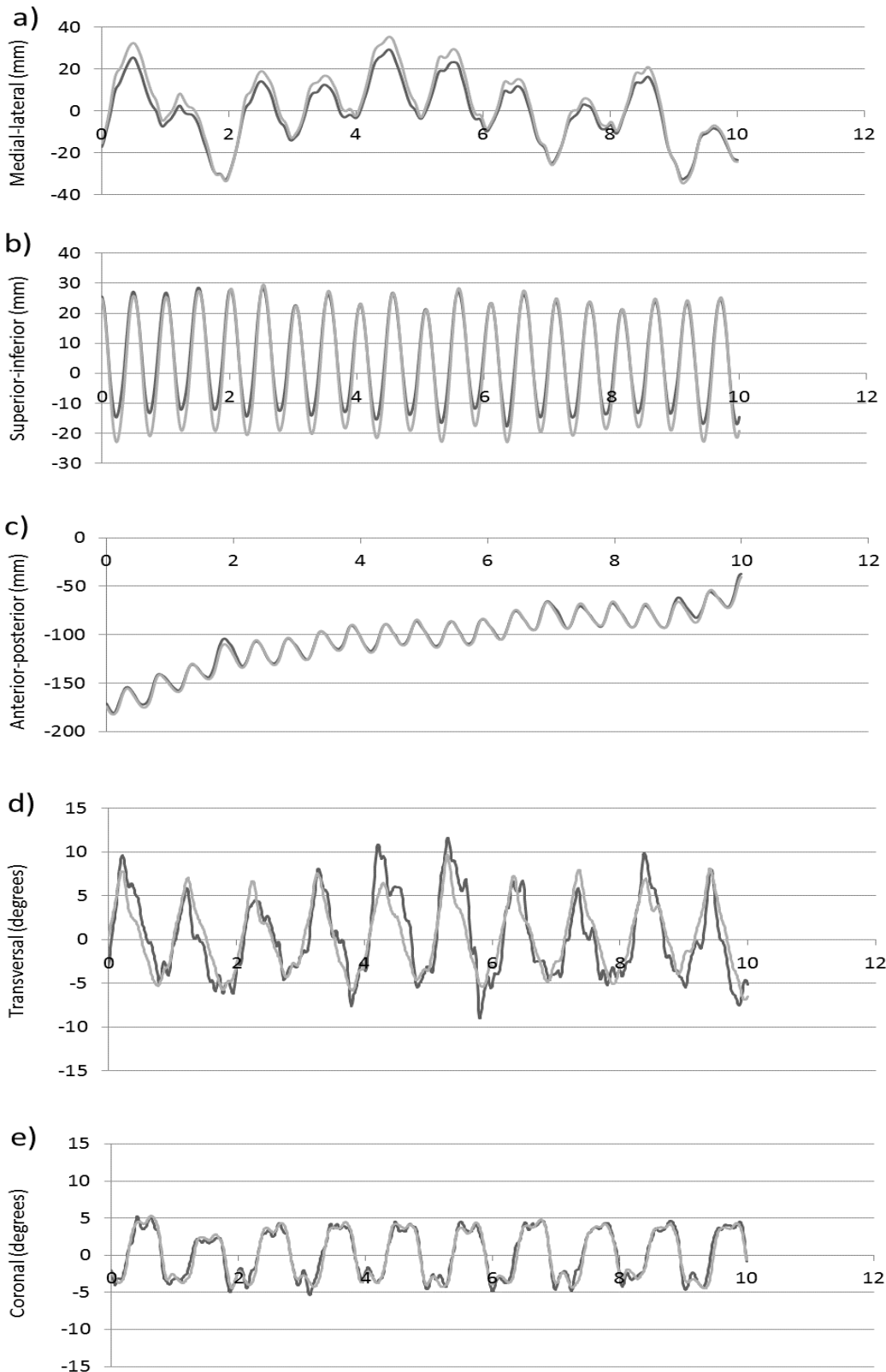
Figure 1. The steps taken to collect data.

315 a) A stationary treadmill was positioned in the six-camera motion capture laboratory. The six cameras
316 were positioned 3m apart surrounding the action. At the rear of the treadmill was the single depth-sensing
317 camera positioned 1.6m above the floor and pointing towards the participant's posterior pelvic region. The
318 participant was fitted with four retro-reflective markers located on the iliac spines and tenth ribs. Also shown are
319 the coordinate systems (right-hand-rule) of the single camera system in grey (X_L , Y_L and Z_L) and the six-camera-
320 system in black (X , Y and Z).

321 b) The resulting infrared image of the 4 markers (i) showing the overexposed pixels and the scanlines
322 used to create the 3-dimensional point cloud around the perimeter of the marker. The resulting point cloud
323 shown from the posterior (ii), lateral (iii) and superior (iv) views. Also shown is the orientation of single-camera
324 local system.

325
326

327



328
 329
 330
 331
 332
 333

Figure 2. Time-series of data points taken over a 10 second interval for self-selected walking in the pelvis of one of the participants. The single depth-sensing camera (black line) and the six-camera system (grey line). Positional data in the medial-lateral (a), superior-inferior (b) and anterior-posterior directions (c). Angular rotations are in the transversal (d) and coronal (e) planes.

Table 1. Within subject correlation coefficients between the six- and one-camera systems, reported with 90% Confidence Limits and the magnitude of correlation coefficient descriptor.

	<i>Linear</i>						<i>Angular</i>			
	Pelvis			Trunk			Pelvis		Trunk	
	Medial-lateral	Anterior-posterior	Superior-inferior	Medial-lateral	Anterior-posterior	Superior-inferior	Frontal	Transversal	Frontal	Transversal
Walking	0.97 (0.93-0.99) <i>Nearly Perfect</i>	0.96 (0.91-0.99) <i>Nearly Perfect</i>	0.92 (0.82-0.97) <i>Nearly Perfect</i>	0.99 (0.96-1.00) <i>Nearly Perfect</i>	0.91 (0.79-0.96) <i>Nearly Perfect</i>	0.88 (0.73-0.95) <i>Very Large</i>	0.41 (0.02-0.69) <i>Moderate</i>	0.41 (0.03-0.69) <i>Moderate</i>	0.57 (0.23-0.79) <i>Large</i>	0.66 (0.36-0.84) <i>Large</i>
70% VIFT	0.98 (0.96-0.99) <i>Nearly Perfect</i>	0.91 (0.78-0.96) <i>Nearly Perfect</i>	0.99 (0.96-1.00) <i>Nearly Perfect</i>	0.99 (0.98-1.00) <i>Nearly Perfect</i>	0.90 (0.76-0.96) <i>Very Large</i>	0.98 (0.96-0.99) <i>Nearly Perfect</i>	0.53 (0.17-0.76) <i>Large</i>	0.62 (0.29-0.81) <i>Large</i>	0.73 (0.47-0.88) <i>Very Large</i>	0.75 (0.50-0.89) <i>Very Large</i>
90% VIFT	0.99 (0.98-1.00) <i>Nearly Perfect</i>	0.89 (0.76-0.96) <i>Very Large</i>	0.95 (0.88-0.98) <i>Nearly Perfect</i>	1.00 (0.99-1.00) <i>Nearly Perfect</i>	0.87 (0.71-0.95) <i>Very Large</i>	0.99 (0.96-1.00) <i>Nearly Perfect</i>	0.61 (0.28-0.81) <i>Large</i>	0.59 (0.25-0.80) <i>Large</i>	0.80 (0.58-0.91) <i>Very Large</i>	0.79 (0.57-0.91) <i>Very Large</i>

334

335

336

337

338

339

340

341

Table 2. Limits of Agreement between the single- and six-camera systems for linear (mm) and angular (degrees) movements (Bias \pm 95% Confidence Intervals)

	<i>Linear (mm)</i>						<i>Angular (degrees)</i>			
	Pelvis			Trunk			Pelvis		Trunk	
	Medial-lateral	Anterior-posterior	Superior-inferior	Medial-lateral	Anterior-posterior	Superior-inferior	Frontal	Transversal	Frontal	Transversal
Walking	-2.0 \pm 1.6	-0.8 \pm 3.9	-3.2 \pm 1.9	-2.1 \pm 1.3	-1.0 \pm 5.0	-3.6 \pm 1.9	-1.1 \pm 2.2	-1.5 \pm 1.2	-4.6 \pm 5.9	-2.2 \pm 4.9
70% VIFT	-2.5 \pm 1.7	-3.4 \pm 6.4	-7.9 \pm 3.0	-3.3 \pm 2.3	-9.4 \pm 7.8	-5.4 \pm 3.0	-1.6 \pm 1.7	-1.1 \pm 1.4	-3.2 \pm 6.5	-0.3 \pm 5.7
90% VIFT	-3.2 \pm 2.7	-3.7 \pm 7.9	-7.7 \pm 2.3	-3.5 \pm 2.0	-9.9 \pm 8.5	-5.6 \pm 2.3	-1.3 \pm 1.5	-1.1 \pm 1.2	-2.2 \pm 5.9	-0.8 \pm 5.3

342

343

344

345

346

347

348

Table 3. Absolute linear (mm) and angular amplitudes (degrees) for the single-camera systems (Mean \pm Standard Deviation)

	<i>Linear</i>						<i>Angular</i>			
	Pelvis			Trunk			Pelvis		Trunk	
	Medial-lateral	Anterior-posterior	Superior-inferior	Medial-lateral	Anterior-posterior	Superior-inferior	Frontal	Transversal	Frontal	Transversal
Walking	50.4 \pm 15.7	39.3 \pm 8.2	46.8 \pm 9.8	55.6 \pm 19.3	35.0 \pm 7.0	48.7 \pm 8.5	10.5 \pm 1.1	6.3 \pm 1.8	15.7 \pm 3.9	9.9 \pm 2.1
70% VIFT	38.6 \pm 11.0	44.6 \pm 6.6	106.7 \pm 12.7	68.0 \pm 15.8	44.1 \pm 7.8	90.6 \pm 9.6	11.6 \pm 2.1	9.3 \pm 2.1	15.4 \pm 3.4	23.5 \pm 6.0
90% VIFT	50.4 \pm 12.1	44.7 \pm 5.7	99.7 \pm 12.6	75.5 \pm 16.9	43.3 \pm 8.2	84.9 \pm 10.5	12.0 \pm 2.1	9.4 \pm 2.2	17.5 \pm 3.8	26.9 \pm 5.9